STOCHASTIC COMPRESSIVE FAILURE SURFACE MODELLING FOR THE UNIDIRECTIONAL FIBRE REINFORCED COMPOSITES UNDER PLAINSTRESS

NABEEL SAFDAR[1*], BENEDIKT DAUM[1] AND RAIMUND ROLFES[1]

[1*] Leibniz Universität Hannover, Institute of Structural Analysis
Appelstr. 9A, D – 30167 Hannover, Germany
n.safdar@isd.uni-hannover.de

Key words: Kinking, Compressive failure, Fibre reinforced composites, Failure surfaces

Abstract. We present a finite element modelling framework to capture the distribution of in-plane compressive failure strengths of unidirectional fibre reinforced composites resulting from the characteristic spatial distribution of fibre misalignments. Using a homogenized fibre-matrix representation of composite, the spread of resulting peak stresses calculated using Monte Carlo simulation led by fibre orientations given at each material point, are used to formulate probabilistic failure surface.

1 INTRODUCTION

Owing to their exceptional properties such as high strength and stiffness to weight ratio, fibre reinforced composites (FRPs) have become an attractive option for use in advanced structural applications, mainly in the fields of aerospace, wind energy and automotive. This class of materials offer environmental benefits from different perspectives. Relatively easier manufacturing processes compared to metals and lightweight construction result in energy and fuel savings. All these advantages are best exemplified by most recent large civil aircrafts such as Airbus A380 and Boeing 747, which are using carbon FRPs for more than half of airframe structure. These structural parts include highly compression loaded components such as fuselage, fins and rudders among others [1, 2].

Because of high compression loads during service time of a structural component, strength under compression is a highly relevant mechanical property. Unidirectional fibre reinforced composites serve the purpose in this regard, but on the other hand compressive failure of these materials is a design limiting phenomenon. Compressive strengths are generally less than 60% of the tensile strengths in industrial composites having ~60% fibre volume fraction [3].

Compressive failure at micro level is predominantly led by microbuckling of fibres in a highly localized band and the phenomenon is called kinking [3]. Considering microbuckling to be caused by elastic loss of stability, Rosen gave the frequently quoted formula (1) [4]:

$$\sigma_c = G_m / (1 \text{-} v_f) \tag{1}$$

where σ_c is the kinking stress which would define compressive strength, G_m is the shear modulus of the matrix and v_f is the fibre volume fraction. Budiansky interpreted Rosen's result as $\sigma_c = G$ which is effective longitudinal composite shear modulus [6].

Argon [5] argued that Rosen formula of buckling of fibres in an elastic matrix gives an upper limit on compressive strength. Argon considered initial fibre misalignments along with

matrix shear strength to play an important role, defining the location and value of kinking stress. Based on this argument of plastic microbuckling mechanism, the well-known formula (2) was given:

$$\sigma_c = \tau_y / \phi_o \qquad (2)$$

where τ_y and ϕ_o are the shear strength of matrix and the initial fibre misalignment respectively. Budiansky [6] extended this approach to a more generalized formulation (3) which asymptotes to Argon's result when the shear yield strain (γ_y) is small compared to initial fibre misalignment:

$$\sigma_c = \tau_y / (\gamma_y + \phi_o) \qquad (3)$$

It was also pointed out that a higher reduction in kinking stress occur for inclined kink bands, which are observed most often experimentally. Two analytical cases of very short and long wavelengths of fibre misalignments were considered to come up with the range of resulting kink band inclination, emphasizing that not only misalignment angle but additionally amplitude affect the resulting strength. All the aforementioned analytical formulations considered an infinite waviness region, meaning that the waviness region stretches across the whole transversal to the nominal fibre direction length of the representative volume element (RVE).

With increasing computational power available in 90s, numerical solution schemes became common. Kyriakides et. al. [7] predicted the compressive strength using a 2D periodic array of imperfect fibres and matrix, in which fibres are modelled as nonlinear isotropic and matrix is considered as an elasto-plastic solid based on J2 plasticity theory. Inspired by their parallel experimental outcomes, parametric numerical analyses were performed using idealized sinusoidal form of fibre misalignment and it was concluded that wavelength and amplitude of waviness have a high impact on predicted strengths. Predicted compressive strength and corresponding strain values were validated, and subsequently substantiated Argon's theory that fibre imperfections indeed play an important role in strength calculations. Prabhakar and Waas [8] performed a numerical study using a micromechanical model of unidirectional plies under in-plane loading conditions. The focus was on the competing mechanisms of kinking and splitting of fibres with virtual variation in material properties to quantify and distinguish these failure mechanisms. It was suggested that modelling should include cohesive elements in cases where splitting failure is equivalently likely to occur as kinking for a better prediction of compressive strength. Recently, Bishara et. al. [9] investigated the mechanisms of kinking failure using 3D numerical micro modelling. Differences between compressive strength of composites having small and large wavelength misalignments were shown as well as the resulting kink band inclination. The following sequence for kinking failure was reported; fibre imperfections induce yielding of the matrix which then propagates to form a yield band with increasing width in nominal fibre direction reaching a specific value. At this point the bent fibres having reduced support in transversal direction through matrix, result in fibre breakage on tensile loaded side of the localized band. This damage propagates towards final failure forming the typical kink band.

In addition to analytical and numerical findings to ascertain compressive strength of FRPs, throughout the past few decades parallel experimental studies have been performed to validate the theoretical results as well as to quantify the effects of different material properties. One of

the first extensive testing of carbon, glass and polyamide fibres embedded in polyester resins with varying combinations was carried out by Piggott and Harris [10]. Although most of the tests were carried out with relatively low fibre volume fractions, the main outcomes were that the matrix shear has a dominant role in characterising compressive strength, and comparatively higher variation in compressive strengths among tests with same specifications. Kyriakides et. al. [7] performed experimental studies on an AS4 carbon fibre reinforced PEEK thermoplastic based composite with 60% v_f to study the effects of fibre imperfections. The tests were performed on flat coupons and cylindrical rod specimens. Even though the testing was performed within carefully controlled conditions, the resulting compressive strengths showed considerable spread.

Since all analytical, numerical and experimental results pointed towards the importance of fibre misalignment in FRPs, there was a need to measure them experimentally. The first effort in this regard was carried out by Yurgartis [11] on a carbon fibre based composite using micrographs and measuring in-plane and out-of-plane misalignments from the images. The fibre misalignment angles were shown to be nearly normally distributed in both in-plane and out-of-plane measurements which were independent of each other. Paluch [12] followed suit with a different methodology by studying sections cut at different regularly spaced locations and visualizing them under optical microscope. The hypothesis that there is no correlation in undulations of neighbouring fibres was challenged and it was shown that fibres undulate with certain interactions to their immediate neighbours. Clark et. al. [13] performed similar studies using confocal laser scanning microscopy and showed similar trend in results. Based on these outcomes, spectral densities of fibre misalignments were calculated.

An important mechanics aspect for small wavelength undulations considered by Fleck et. al. [14, 15] was that of fibre bending resistance. Using couple stress theory and a Ramberg-Osgood solid description in shear and transverse direction on a homogenized description of fibre-matrix composite material, kink band width and the factors controlling the initiation and growth of kink band were explained. The results confirm that compressive strength is affected most by initial fibre misalignment and to a lesser extent by the longitudinal width of this initial band of misaligned region. Based on the realization of variation of misalignment from experimental outcomes, Slaughter and Fleck [16] extended their couple stress theory based approach to add the effects of random fibre waviness on compressive strength using a homogenized continuum definition of fibre-matrix composite material and by performing Monte Carlo simulation. Liu et. al. [17] later extended it to 2D and fitted the resulting distribution of compressive strength with a Weibull distribution. A weakest link based engineering approach was subsequently proposed to estimate axial compressive strength from the aforementioned results. Another notable contribution is from Allix et. al. using a hybrid micro-model. This was a damage based continuum cell approach in which cells, representing a homogenized fibre-matrix material and having a random uncorrelated material orientation depicting fibre misalignments, were engulfed in cohesive zone elements representing potential fracture surfaces. The length of the cells was directly related to ply thickness and corresponding experimentally deducted kink band widths. The model was used to demonstrate kink band formation and its interaction with other failure mechanisms under compression [18]. An interesting work to incorporate the randomness of fibre misalignment into material characteristics prediction is from Bednarcyk et. al. [19] Through High-Fidelity Generalized Method of Cells Micromechanical Model (HFGMC) and probability-weighted

averaging of the appropriate stress concentration tensor of the subcell based on probability density function representation of fibre misalignments, effective material moduli and damage initiation envelopes under varying input properties were predicted.

Even though mechanical properties of FRPs, especially under compression loading, vary a great deal, the general focus of most analytical and numerical, and consequently, experimental studies have been on prediction of a deterministic strength value under compression with few exceptions. This variation in strength causes the engineers to use high factors of safety, thus affecting costs and efficient use of material. In order to better utilize the exceptional mechanical properties of FRPs, there is a need to do further research in quantifying this spread of compressive strength. One of the examples in this regard is that of Curtin [20] who provided a stochastic model for tensile damage evolution. Basu et. al. [21] used an analytical formulation with an idealized form of waviness to predict the compressive failure under multi-axial loading. Failure envelopes for strength under compressive load along with transverse compression and shear were also predicted.

In this contribution a relatively simple finite element methodology is employed to capture the variation in strength values under in-plane loading conditions, with fibre misalignment modelled stochastically following the approach of Liu et. al. [17]. Using this homogenized fibre-matrix representation technique, the so called idealized form of infinite band fibre misalignment or waviness has also been simulated to help interpret results. After performing mesh and effective RVE studies, in-plane probabilistic failure surfaces are generated which could help in representation of microstructure variation in macro structural response.

2 METHODOLOGY

2.1 Material model

Most of the analytical and numerical approaches [4-9] consider separate material models of elastic fibres embedded in an elasto-plastic resin. This approach, even though computationally expensive and difficult to model with realistic fibre misalignments, is the method of choice if the target is to predict interactions between different failure mechanisms under certain conditions. However, this study focuses on the probabilistic effects of fibre misalignment on strength predictions, therefore, it is advantageous because of easier modelling to use a homogenized material model representing fibre-matrix composite as a single anisotropic material as shown by Liu et. al. [17].

Fleck et. al. [14] showed that for small wavelengths of fibre misalignments, fibre bending stiffness plays an important role in determining the compressive strength as it increases the resulting predicted strength of the composite. However, when the wavelengths are large, which is often the case in industrial composites, the results of their couple stress theory modelling and kinking theory of Budiansky [6] converge to the same value. Hence, the role of fibre bending stiffness is neglected in this work.

Anisotropic elasticity is modelled using homogenized properties based on Voigt micromechanical theory. Elastic material properties are taken from Kaddour et. al. [22] and are listed in Table 1. Plasticity is modelled using Hill's potential function with an associative plastic flow rule [23]. Even though this plasticity model is aimed for anisotropic metal plasticity, it can still be employed here effectively to detail the methodology under in-plane loading conditions provided certain modifications because long fibre CFRPs only show

plasticity in shear and transverse directions. This is achieved by adjusting appropriate constants of yield surface definition in the model. The nominal fibre direction coincides with the 1 direction and as CFRP show no plastification in fibre direction, therefore, yielding is eliminated in this load direction. The yield criterion is of the form:

$$2f(\boldsymbol{\sigma}) = (\sigma_{22}/2Y)^2 - (\sigma_{11}\sigma_{22}/Y)^2 + (\tau_{12}/S)^2 \tag{4}$$

where Y and S are transverse and shear yield stresses respectively. Non-linear isotropic hardening is specified and subsequently mapped to anisotropy by Hill's parameters. The fact that kinking failure is controlled by shear response of the matrix, the input data of hardening is chosen for in-plane shear hardening curve, taken from Vogler et. al. [24]. For this purpose commercial software Abaqus is employed. An extension to 3D modelling using pressure-dependent material model and with 3D yield surfaces based on experimental data is planned in the follow-up work.

Table 1: Mechanical properties of unidirectional IM7/8552

Property	Value
Longitudinal modulus E_1 (GPa)	171
Transverse modulus E_2 (GPa)	8.9
In-plane shear modulus G_{12} (GPa)	5.6
Major Poisson's ratio υ_{12}	0.34

2.2 Waviness Distribution

Idealized waviness:
An idealized sinusoidal infinite band form of waviness in a localized region was used following Bishara et. al. [9] to help better understand the kink band formation for homogenized fibre-matrix composite material modelling approach.

Random waviness:
Experimental data has shown that fibre misalignment is in fact stochastic in nature in engineering unidirectional FRPs [11, 12, and 13]. It has been measured and calculated to exist randomly with certain characteristic parameters over the whole volume with a Gaussian distribution.

Liu et. al. [17] following Slaughter and Fleck [16] used the concept of signal processing theory to model the spatial distribution of fibre misalignments from spectral density functions of fibre slope $\alpha = \tan(\phi)$. Analysing the spectral density plots generated from experimental data by Clark et. al. [13], Liu. et. al [17] argued that it is reasonable to use the exponential function for 2D spectral density of fibre slope given in the form:

$$S(\omega_x, \omega_y) = S_o e^{-((\omega_x/\omega_{cx})2 + (\omega_y/\omega_{cy})2)} \tag{4}$$

where ω_{cx} and ω_{cy} and are cut-off frequencies in x and y spatial directions and S_o is initial spectral density. Graph of spectral density using the exponential fitting equation (4) in *xy* plane is shown in Figure 1. In order to perform Monte Carlo simulation random waviness distribution are generated. The algorithm used is the one given by Liu et. al. [17] in which

spectral density is sampled using eq. 4 and through inverse fourier transform with random phase angles, random waviness distributions were generated.

The resulting spatial distribution of fibre misalignments on a sample RVE is shown in Figure 2. A fibre is also tracked on top of it. Black lines represent misaligned fibres whereas red line is 7x zoomed version of the same fibre. One can easily see the randomness of the fibre misalignments with regions of positive and negative slopes based on the underlying wavelengths superimposed in spatial domain.
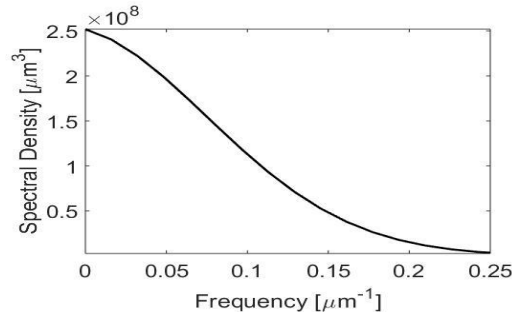
Figure 1: Spectral density of fibre slopes in *xy* plane
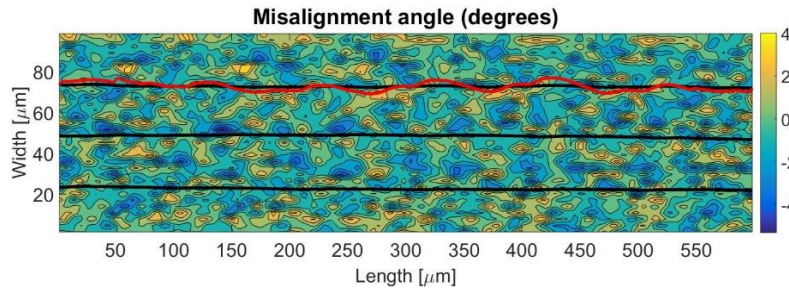
Figure 2: Fibre misalignment distribution

2.3 Geometrical Modelling

Figure. 3 illustrates the schematics of the model which is in the form of a quadrilateral. Nominal 0° fibre direction is parallel to x-axis of the model. The nodes on left hand side are constrained in x-direction and bottom left node is constrained additionally in y-direction to avoid rigid body motions. The nodes on the right edge are coupled to a reference node. Loads are applied on the reference node in the form of concentrated forces resulting in compressive and shear loads in respective models. For all the models, two dimensional plane stress 8 node reduced integration elements (CPS8R) are used. A structured mesh with square dimensions was used in all models whether with random or idealised waviness, or with square or rectangular models. Thorough mesh and RVE convergence studies have been performed and the model dimensions are discussed later in the respective subsection of the following results section. The orientations were generated using the algorithm given in Liu et. al. [17] and were applied on material point of each finite element to represent the local material direction. Because each element has a single fibre orientation, this allows to represent the realistically varying local material direction in unidirectional FRPs arising due to fibre misalignments.

6

Since under predominant compression, the failure is driven by plastic microbuckling which is caused by geometrically non-linear deformation. Hence, a geometrically non-linear implicit solution is carried out. With idealised form of waviness, snap-back after the peak load is tracked using Riks' algorithm. In other simulations for RVE and failure surface studies, the same can be achieved. But since the focus is only on the peak loads for these, the analysis is terminated after the peak load has been reached.
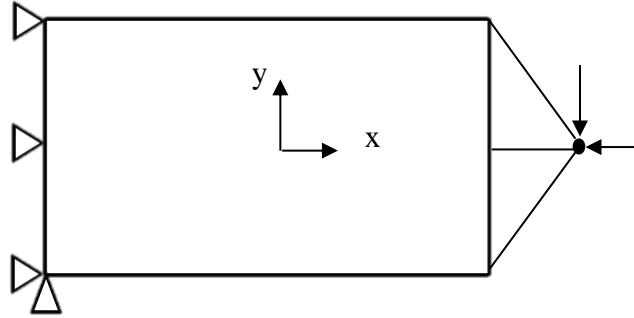

Figure 3: Model Schematic

3   RESULTS

3.1 Mesh Sensitivity

Finite element analysis requires a proper discretization of the geometry based on results' accuracy and computational costs. Another aspect to keep in mind is that since fibre orientation is assigned to each integration point within each finite element, this would also drive how refined the fibre misalignment distribution representation is. Additionally, since this study is based on capturing variation on compressive strength resulting from probabilistic fibre misalignments, it was deemed necessary to perform a mesh sensitivity analysis in a probabilistic manner. For this purpose a square RVE with dimensions of 100µm was chosen and 500 realization have been simulated for each mesh size with successive mesh refinement. Initial discretization was 4 elements in each dimension of the square model, and for each refinement mesh size was halved resulting in four times the number of elements in 2D model in each consecutive refinement.

The results of mesh refinement are plotted in Figure 4. showing axial compressive peak stress (axial load at reference node per initial model cross-sectional area) against the number of elements of the respective model. Vertical lines represent the spread of resulting compressive stress values, and the corresponding mean and first standard deviation from the mean highlighted with dots on these vertical lines. The convergence of mean values shown by the red line, as well as overall spread of the data visible by standard deviation points, asymptotes after 4th refinement. Hence, this mesh density of 3.125µm mesh edge length is chosen which corresponds to roughly half the diameter of fibre diameter. This size of discretization is also logical as it represent the fibre misalignment distribution in detail.
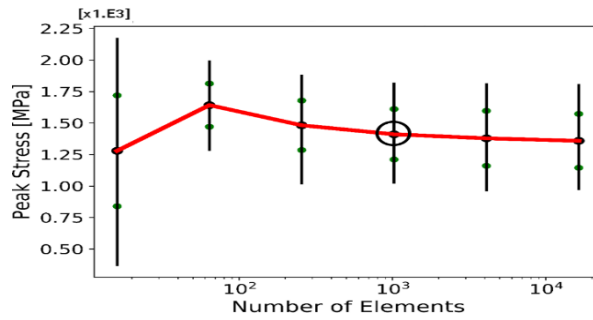
Figure 4: Mesh Sensitivity Study

3.2 Idealised Waviness vs Random Waviness

In order to highlight the need to model the spatial distribution of misalignment over whole domain, it is considered necessary to plot axial stress strain curves from same model dimensions (500µm×100µm) using both approaches i.e. idealized sinusoidal and random waviness, see Figure 5. Up to peak load, both modelling approaches predict a linear response with the same slope. The value of peak stress from the idealized sinusoidal model of fibre misalignment is different from the one where misalignment is modelled over the whole spatial domain as expected. The value of peak stress from random waviness models show a distribution rather than a deterministic value, which is presented in section 3.4. In other realizations of random waviness, peak stress could be either higher, lower or same as the deterministic value of idealized waviness model.
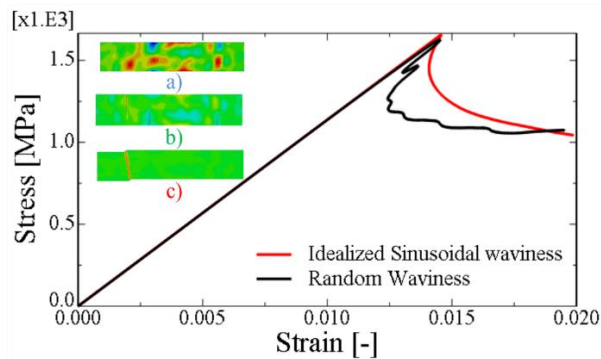

**Figure 5**: Longitudinal stress against longitudinal strain

The snap back response under axial compression load can be easily predicted using a homogenized modelling approach as depicted. The differences in snap back path between two approaches arise from the fact that when waviness is spatially distributed, there are competing kink bands giving rise to small peaks and troughs in post peak stress part of the curve. Finally, the most critical of these kink bands, based not only on amplitude and size of the waviness but also on its location relative to neighbours deciding whether they aid or hinder its propagation, matures and spread across the width. This phenomenon can be observed though the contour plots of the in-plane shear stress distribution of the model shown at three location of stress-strain curve: a) at first loading sub-step, b) at peak load, and c) at the point of final failure.

8

Budiansky formula (3) gives a compressive strength value of 1650MPa with misalignment angle of 2.5°, which is very similar to the one calculated of 1657MPa for idealized sinusoidal model having maximum misalignment 2.5°. Therefore, it is concluded that this approach gives accurate results. The particular random waviness realization gives a compressive strength value of 1625MPa. This realization is generated with misalignment angles in the range -3° to +3° and is not an outlier in terms of peak compressive stress distribution.

3.3 RVE Study

The need to select an appropriate RVE first is a vital step. There are different factors controlling the selection of an appropriate RVE for the proposed approach which are certain aspect ratios of RVE length to width to avoid global buckling, feasible computational time and total size defining the size of misalignment wavelengths inclusion in the distribution. Hence, a suitable RVE size for prediction of the in-plane strength properties is the one which would provide an optimum of all the aforementioned aspects. For this purpose a detailed RVE size study has been performed with sizes ranging from 50µm to 2000µm. The aspect ratio ranges from 0.2-5 as this range avoids global buckling and the peak stresses result from kink band initiation. Another aspect to consider is the fibre misalignment distribution for each size. Since it is impractical to perform Monte Carlo simulations for each size to find the peak stress distributions, it was assumed that if the realizations are generated randomly for all sizes, the resulting fitting would result in the mean surface.

The results are plotted in the form of a surface. The base plane represents model dimensions i.e. length (x) and width (y) respectively and height is given by the respective peak stress of the model, see Figure 6 a). The resulting data was fitted to a surface using a 2nd degree polynomial in both x and y with least absolute residuals (LAR) method. LAR gives equal weight to all data points. On very small models, the deviation in the results is very high as expected. The reason is that if the model size is too small, it will not represent typical fibre misalignment distributions and thus, susceptible to outliers. Secondly, edge effects are too high in such models thus the peak stress in model is attained sooner in most cases. As the model size is increased, the spread of data becomes shorter which is visible through a residual plot, Figure 6 b), showing the distance of each data point to the fitted surface. The minimum point after which the changes in surface are less sudden and the respective residuals are minimal is chosen and it corresponds to a model length of 1000µm and a width of 500µm. Hence, this model was used for the next phase of probabilistic failure surface study.
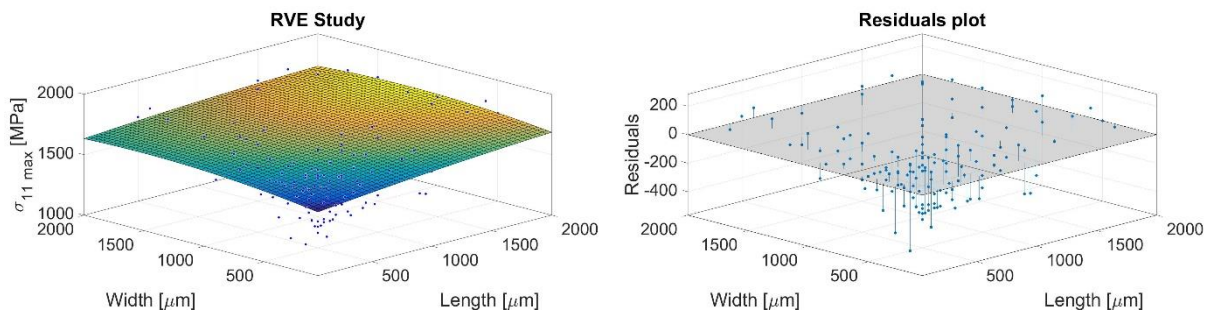
Figure 6: RVE Study a) Polynomial surface fitting, and b) Residuals plot from the fitting

3.3 Probabilistic In-plane Failure Surface

After selecting the appropriate RVE, simulations have been performed for several loading combinations to construct a failure surface. Different systematic proportional load combinations of axial and shear loads applied at the reference node of the model has been chosen to obtain distributions of peak stresses at each loading scenario. For each load case a fixed convergence criteria of max 1% and 1.5% change in mean and standard deviation after 15 realizations was used. Convergence was achieved in 90-120 realizations for each load case.

The results of the distribution of each load case using Monte Carlo simulation are plotted in Figure 7 a). Small black lines in each loading direction represent whole distribution whereas blue boxes on top are representative of 1 standard deviation (red and green dots) from mean (yellow dots). As the mean values of peak stress at each load case show a linear trend, they are fitted with a linear failure surface, eq. 5. It can be seen that the maximum compressive load carrying capacity is highly sensitive to even small applied shear loads as it adds to the shear deformation of the matrix by fibre rotation, speeding the kink band formation. The shape of the failure surface using the current approach corresponds to the one presented by Basu et. al. [21]. A major aspect to be noted is that with the current approach, the failure surface is symmetric with respect to shear loads whereas the one from Basu et. al. is asymmetric. Since they used an idealized form of waviness which pre determines the direction of fibre rotation, therefore, the shear load either increase fibre rotation or it can straighten up fibres. In reality there is no single misaligned region which would show the said behaviour. Fibres are misaligned randomly, therefore, shear loadings tend to support the rotation of fibres resulting in reduction in compressive strength. Another aspect to be noted is that with increasing shear and proportionally decreasing axial compression, the distribution of the peak stress tend to shorten. This can be seen by the standard deviation of each load case in Figure 7 b). Standard deviation are fitted to a quadratic function, eq. 6 and the fitting parameters are given in Table 2. Since in pure shear, fibres do not support the load hence, at this point standard deviation almost vanishes.

$$F_m = 1 + f_1\sigma_{11} + f_2\tau_{12} \tag{5}$$

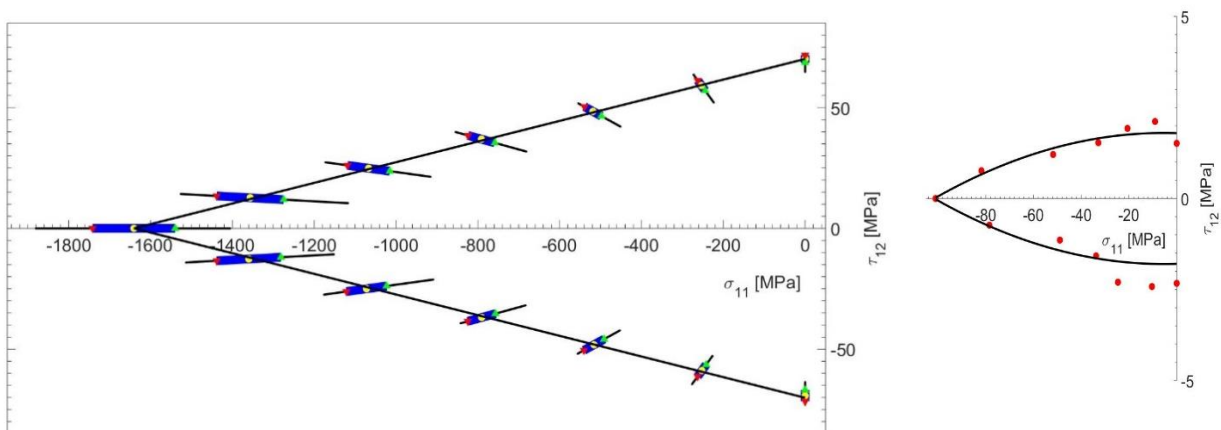$$F_{std} = -1.794 + f_1(\sigma_{11})^2 + f_2\sigma_{11} + \tau_{12} \tag{6}$$

Figure 7: a) Probabilistic failure surface, and b) Corresponding standard deviations

10

Table 2: Fitting parameters

Function	f_1	f_2
Mean of peak stress eq. 5	1640	70
Standard deviation of peak stresses eq. 6	1.945e-04	2.0813e-03

4 CONCLUSION AND OUTLOOK

The effects of random fibre waviness on in-plane failure surface of fibre reinforced composites has been explored using finite element method using a homogenized representation of fibre-matrix composite material. The differences between the post peak behaviour of idealized and random form of waviness have been highlighted and compared to well-known Budiansky [6] formula. A detailed RVE study over a large range of model sizes to find the optimum RVE was accomplished. Furthermore, the concept of probabilistic failure surfaces using the current approach has been demonstrated. The results confirm that compressive strength is highly sensitive to applied shear loads. The shape of the failure surface is in accordance with the one shown by Basu et. al. [21]. In the follow-up work, 3D probabilistic failure surfaces under multi-axial loadings will be presented. Size effect studies and upscaling from micro to macro results are also to follow.

ACKNOWLEDGMENTS

REFERENCES

[1] Soutis, C. *Fibre reinforced composites in aircraft construction.* Progress in Aerospace Sciences (2005) **41,** no. 2 143-151.

[2] Jerome, P.O. *Composite materials in the airbus A380-from history to future.* http://www.iccm-central.org/Proceedings/ICCM13proceedings/SITE/PAPERS/paper-1695.pdf (2001)

[3] Budiansky, B. and Fleck, N.A. *Compressive kinking of fiber composites: a topical review.* Applied Mechanics (1994) Reviews 47, no. 6S 246-250.

[4] Rosen, B. W. *Mechanics of composite strengthening.* (1965)

[5] Argon, A.S. *Fracture of composites.* Treatise of Materials Science and Technology (1972) 1:79 - 114

[6] Budiansky, B. *Micromechanics.* Computers & Structures (1983) **16**(1-4), 3-12

[7] Kyriakides, S., Arseculeratne, S., Perry, E.J. and Liechti, K.M. *On the compressive failure of fiber reinforced composites.* International Journal of Solids and Structures (1995) **32**, no. 6-7 689-738.

[8] Prabhakar, P. and Waas, A.M. *Interaction between kinking and splitting in the compressive failure of unidirectional fiber reinforced laminated composites.* Composite Structures (2013) **98** 85-92.

[9] Bishara, M., Rolfes, R. and Allix, O. *Revealing complex aspects of compressive failure of polymer composites–Part I: Fiber kinking at microscale.* Composite Structures (2017) **169** 105-115.

[10] Piggott, M.R. and Harris, B. *Compression strength of carbon, glass and Kevlar-49 fibre reinforced polyester resins.* Journal of Materials Science (1980) **15**, no. 10 2523-2538.

[11] Yugartis, S.W. *Measurement of small angle fibre misalignments in continuous fibre composites.* Composite Science and Technology (1987) **30**, no. 4 279-293.

[12] Paluch, B. *Analysis of geometric imperfections affecting the fibers in unidirectional composites.* Journal of composite materials (1996) **30**, no. 4 454-485.

[13] Clarke, A.R., Archenhold, G., Davidson, N.C., Slaughter, W.S., and Fleck, N.A. *Determining the power spectral density of the waviness of unidirectional glass fibres in polymer composites.* Applied Composite Materials (1995) **2**, no. 4 233-243.

[14] Fleck, N.A., Deng, L., and Budiansky, B. *Prediction of kink width in compressed fiber composites.* Journal of Applied Mechanics (1995) **62**, no. 2 329-337.

[15] Fleck, N.A., and John Y.S. *Microbuckle initiation in fibre composites: a finite element study.* Journal of the Mechanics and Physics of Solids (1995) **43**, no. 12 1887-1918.

[16] Slaughter, W.S., and Fleck, N.A. *Microbuckling of fiber composites with random initial fiber waviness.* Journal of the Mechanics and Physics of Solids (1994) **42**, no. 11 1743-1766.

[17] Liu, D., Fleck, N.A., and Sutcliffe, M.P.F. *Compressive strength of fibre composites with random fibre waviness.* Journal of the Mechanics and Physics of Solids (2004) **52**, no. 7 1481-1505.

[18] Allix, O., Feld, N. Baranger, E., Guimard, J-M., and Ha-Minh, C. *The compressive behaviour of composites including fiber kinking: modelling across the scales.* Meccanica (2014) **49**, no. 11 2571-2586.

[19] Bednarcyk, B.A., Aboudi, J., and Arnold, S.M. *The effect of general statistical fiber misalignment on predicted damage initiation in composites.* Composites Part B: Engineering (2014) **66** 97-108.

[20] Curtin, W.A. *Stochastic damage evolution and failure in fiber-reinforced composites.* Advances in applied mechanics (1998) **36** 163-253.

[21] Basu, S., Waas, A.M., and Ambur, D.R. *Compressive failure of fiber composites under multi-axial loading.* Journal of the Mechanics and Physics of Solids (2006) **54**, no. 3 611-634.

[22] Kaddour, A.S., Hinton, M.J., Smith, P.A., and Li, S., *Mechanical properties and details of composite laminates for the test cases used in the third worldwide failure exercise.* Journal of Composite Materials (2013) **47** 20-21:2427-2442.

[23] Hill, R. *A theory of the yielding and plastic flow of anisotropic metals.* Proceedings of the Royal Society London (1948) **193** 1033 281-297.

[24] Vogler, M., Rolfes, R., and Camanho, P.P. *Modeling the inelastic deformation and fracture of polymer composites–Part I: plasticity model.* Mechanics of Materials (2013) **59** 50-64.